

# A chemical potential for light

M. Hafezi, P. Adhikari, J. M. Taylor<sup>1</sup>

<sup>1</sup>*Joint Quantum Institute, NIST/University of Maryland, College Park, MD 20742*

Photons are not conserved in interactions with other matter. Consequently, when understanding the equation of state and thermodynamics of photons, while we have a concept of temperature for energy conservation, there is no equivalent chemical potential for particle number conservation. However, the notion of a chemical potential is crucial in understanding a wide variety of single- and many-body effects, from transport in conductors and semi-conductors to phase transitions in electronic and atomic systems. Here we show how a direct modification of the system-bath coupling via parametric oscillation creates an effective chemical potential for photons even in the thermodynamic limit. Specific implementations, using circuit-QED or optomechanics, are feasible using current technologies, and we show a detailed example demonstrating the emergence of Mott Insulator-superfluid transition in a lattice of nonlinear oscillators. Our approach paves the way for quantum simulation, quantum sources and even electron-like circuits with light.

## 1. INTRODUCTION

The study of the thermodynamics of photons dates back to Plank<sup>1</sup>. Investigating blackbody radiation, he realized photons decay due to absorption into walls of their container, and therefore, no chemical potential appeared in his expression, in contrast to Gibbs's thermodynamic expressions for other particles using the grand canonical ensemble. Later, it was understood that in the absence of absorbing walls, photon can acquire non-zero chemical potential, e.g. photon emission in semiconductors (LED)<sup>2</sup>, and thus the useful concept of chemical potential can start to be applied to these systems<sup>3-5</sup>. Moreover, if photons are confined in a cavity and coupled to excitons, they form polaritons which also can thermalize<sup>6</sup>. More recently, it was shown that photons can thermalize with a non-zero chemical potential and form a Bose-Einstein condensate<sup>7-10</sup> when interacting with a nonlinear medium. However, finding a general solution to creating a chemical potential for light remains an open problem<sup>11</sup>.

At the same time, photons provide an intriguing quantum degree of freedom for implementing quantum simulators<sup>12-17</sup> and observing quantum phases of matter<sup>18</sup>. In quantum simulation, one develops a quantum system with a controlled, known Hamiltonian, enabling simulation of problems that are exponentially difficult on a classical computer. This new paradigm covers a wide range of problems from chemistry<sup>19</sup> and quantum field theories<sup>20</sup> to strongly correlated electron systems, such as High- $T_c$  superconductors<sup>21</sup>. However, most phenomena that are interesting from quantum simulation perspective involve thermalization in systems with particle number conservation, i.e., with a controllable chemical potential, as a key parameter in phase diagrams. Both are absent for photons. More specifically, on the one hand, there is no mass for photons giving them a zero chemical potential, and on the other hand, due to the weakness of inelastic scatterings, photons do not naturally thermalize, in contrast to interacting systems.

Here, we propose a general scheme to solve the issue

of chemical potential and thermalization in photonic systems, extending preliminary concepts<sup>22</sup> and developing simpler approaches than current theory<sup>23-25</sup>. In particular, by parametrically coupling a photonic system to a thermal bath, we show that a photonic system can equilibrate to the temperature of the bath, with a chemical potential given by the frequency of the parametric coupler. We apply our scheme to two platforms, circuit-QED and optomechanical systems, where recent and spectacular progress has been made in controlling and using them in a few quanta regime. Finally, we conclude by considering how a photonic lattice implementing a Bose-Hubbard model can be driven through the Mott Insulator-Superfluid (MI-SF) transition<sup>26</sup> using this approach even in the presence of finite dissipation.

## 2. PARAMETRIC THERMALIZATION

We can understand thermalization via a system-bath picture, where the system of choice with Hamiltonian  $H_S$  is coupled via  $\lambda H_{SB}$  to a bath with Hamiltonian  $H_B$  and initial state  $\rho_B \propto \exp(-\beta H_B)$ <sup>27</sup>. Our scheme will follow this approach with one small modification: replace the coupling with a parametric coupling via  $\lambda \rightarrow 2\lambda \cos(\omega_p t)$ , that is, we consider

$$H = H_S + 2\lambda \cos(\omega_p t) H_{SB} + H_B . \quad (1)$$

again with initial conditions  $\rho_B \propto \exp(-\beta H_B)$ . The parametric coupling will enable up- and down-conversion of bath excitations to photons, which will lead to a controlled chemical potentials.

To see this explicitly, we will assume that  $H_{SB}$  is bilinear, of the form

$$H_{SB} = \sum_j (\hat{a}_j + \hat{a}_j^\dagger) B_j \quad (2)$$

where  $\hat{B}_j$  is a bath operator and there exists  $\hat{a}_j, n_j$  such that  $[\hat{a}_j, n_j] = \hat{a}_j$ , as occurs naturally for photons. This property defines particle numbers  $n_j$  and total particle number  $\hat{N} = \sum_j n_j$ .

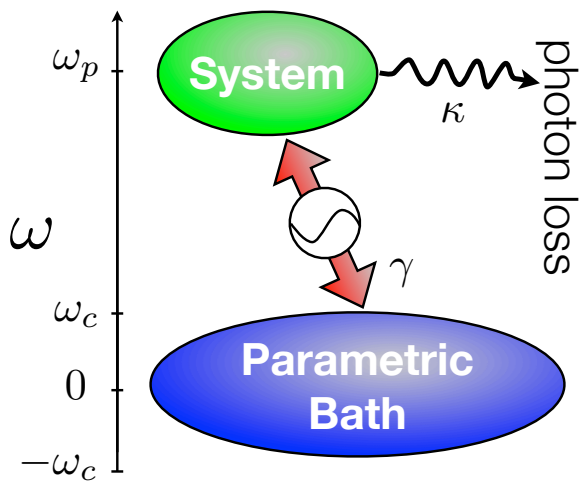


Figure 1: (a) a thermal bath with modes  $\hat{b}_j$  and response functions with a cutoff  $\omega_c$  can be parametrically coupled to a higher frequency (optical) system with modes  $\hat{a}_j$  near the frequency  $\nu_p$ . Additional loss via the high frequency bath can lead transport from the parametric bath through the system to the high frequency bath.

Let us consider what happens when the energy scales of the bath are small compared to  $\omega_p$ , but the energy scales of the system are not. Furthermore, we will decompose  $H_S$  into  $H'_S + H_{S,\perp}$  where  $H_{S,\perp}$  includes all terms that do not commute with the total number of particles in the photonic system, given by  $\hat{N} = \sum_j \hat{a}_j^\dagger \hat{a}_j$ . In this regime, we move to a rotating frame with the unitary transformation  $U = \exp(-it\omega_p \hat{N})$ . The transformed system Hamiltonian becomes

$$U^\dagger H_S U - i\hbar U^\dagger \dot{U} \approx H'_S - \hbar\omega_p \hat{N}. \quad (3)$$

where we have neglected  $U^\dagger H_{S,\perp} U$  by making the rotating wave approximation (RWA), requiring  $\|H_{S,\perp}\| \ll \hbar\omega_p$ .

Meanwhile, the bath Hamiltonian remains the same, while the system bath coupling terms become

$$\left[ \hat{a}_j + \hat{a}_j^\dagger + (e^{-2i\omega_p t} \hat{a}_j + e^{2i\omega_p t} \hat{a}_j^\dagger) \right] B_j \approx \left[ \hat{a}_j + \hat{a}_j^\dagger \right] \hat{B}_j \quad (4)$$

The key approximation is again the RWA to neglect  $e^{2i\omega_p t} \hat{a}_j^\dagger$ -type terms, consistent for a bath whose two-point bath correlation function  $\langle B_i(t + \tau) B_j(t) \rangle$  has a cutoff frequency  $\omega_c < \omega_p$ . This provides our definition of a low frequency bath for this paper, with  $H'_{SB} \equiv \sum_j \left[ \hat{a}_j + \hat{a}_j^\dagger \right] \hat{B}_j$  the system-bath coupling in the RWA.

Through this set of transformations, and the rotating wave approximation, we have a new system-bath Hamiltonian which takes the traditional form

$$H = H'_S - \mu \hat{N} + \lambda H'_{SB} + H_B \quad (5)$$

where we identify  $\mu \equiv \hbar\omega_p$  as the chemical potential. For weak coupling  $\lambda$  and an infinite bath at inverse temperature  $\beta$ , we expect the system to thermalize in the

long-time limit to a density matrix

$$\rho \approx \exp \left[ -\beta (H'_S - \mu \hat{N}) \right], \quad (6)$$

i.e., the distribution is exactly that of the grand canonical ensemble.

The key idea of our approach is to parametrically couple a low-temperature, low frequency bath to a set of high frequency modes. The parametric coupler up-converts bath excitations to photons and down-converts photons to bath excitations, as shown in Fig. 1. This leads to thermalization of photons, as long as the bath thermalization rate and the coupling rate between the bath and photons is faster than other photonic decay rates. These other decay processes can be accounted for by splitting the bath into a high frequency (loss) part and a low frequency (parametric bath) part, and making the RWA only for the latter half. A natural consequence of this two-bath model is that the system will in general be only near equilibrium, as particles will flow from one bath to the other through the system.

### 3. IMPLEMENTATIONS

Now we show that such a scheme, which provides both thermalization and a finite chemical potential for photons, can be implemented in circuit-QED systems for microwave domain photons and using optomechanics for optical domain photons. Following Caldeira-Leggett model, in the context of circuits<sup>28,29</sup>, we consider the bath to be a collection of transmission lines which can be described by a quasi-continuum of harmonic oscillators. The bath Hamiltonian is given by

$$H_B = \sum_\nu \hbar\omega_\nu \left( \hat{b}_\nu^\dagger \hat{b}_\nu + \frac{1}{2} \right), \quad (7)$$

where  $\hat{b}_\nu^\dagger$  is the creation operator of an electromagnetic field quantum at mode  $\nu$  with frequency  $\omega_\nu$ . We assume that the transmission lines are in thermal equilibrium, and thus,  $\langle \hat{b}_\nu^\dagger \hat{b}_{\nu'} \rangle = \frac{1}{e^{\hbar\omega_\nu/k_B T} - 1} \delta_{\nu,\nu'}$ . We consider that each mode of the photonic system is coupled to the bath using non-degenerate parametric amplifiers, through three-wave mixing. While many configurations can implement this concept, we focus on the conceptually cleanest case: a Josephson parametric amplifier in a Wheatstone bridge configuration<sup>30</sup>, as depicted in Fig. 2.

Examining the details of the JJ-Wheatstone parametric coupler, we assume that each junction has a large area, and hence, a large capacitance, so that its charging energy can be ignored. In this approximation, the energy  $U$  of the JJ-Wheatstone bridge is<sup>31</sup>

$$-4E_J \left[ \cos \left( \frac{\Phi_x}{4\varphi_0} \right) \cos \left( \frac{\Psi_X}{2\varphi_0} \right) \cos \left( \frac{\Psi_S}{2\varphi_0} \right) \cos \left( \frac{\Psi_Z}{2\varphi_0} \right) + \sin \left( \frac{\Phi_x}{4\varphi_0} \right) \sin \left( \frac{\Psi_X}{2\varphi_0} \right) \sin \left( \frac{\Psi_S}{2\varphi_0} \right) \sin \left( \frac{\Psi_Z}{2\varphi_0} \right) \right]$$

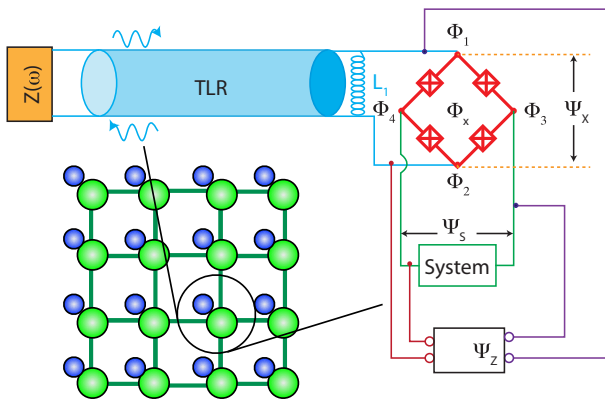


Figure 2: A coupled array of nonlinear microwave cavities provides a potential quantum simulator, where individual elements' parametric coupling to a bath provides chemical potential. The inset shows the bath coupler implementation suggested in the text using circuit QED. Specifically, a transmission line is coupled to the mode  $\Psi_X$  of the coupler. The system is connected to the mode  $\Psi_S$ . The mode  $\Psi_Z = \lambda\Phi_0 \cos \omega_p t$  is driven harmonically at frequency  $\omega_p$  and provides the up- and down-conversion necessary for particle and hole exchange with the bath.

where we have taken all four JJ's to have the same  $E_J$ , and  $\varphi_0 = \Phi_0/(2\pi)$ ,  $\Phi_0 = h/(2e)$  being the superconducting flux quantum. Setting  $\Phi_x = \Phi_0/2$  by choice of flux bias, and assuming the mode intensities  $\Psi_X, \Psi_S, \Psi_Z \ll \Phi_0$ , consistent with moderate to low characteristic impedance circuits, we can expand  $U$  in  $\psi_i = \Psi_i/\Phi_0$ ,  $i \in \{X, S, Z\}$  to third order<sup>32</sup>:

$$U = -2\sqrt{2}E_J + M(\psi_X^2 + \psi_S^2 + \psi_Z^2) + g\psi_X\psi_S\psi_Z. \quad (8)$$

Here  $M = \sqrt{2}E_J\pi^2$  and  $g = -2\sqrt{2}E_J\pi^3$ .

A transmission line resonator (TLR) is connected inductively to the coupler mode  $\Psi_X = \Phi_1 - \Phi_2$  through inductance  $L_1$ . The modes, assumed to be in thermal equilibrium at a temperature  $T$ , act as a bath. The (microwave) photonic system is coupled to the mode  $\Psi_S = \Phi_4 - \Phi_3$  while the mode  $\Psi_Z = \Phi_1 - \Phi_3 + \Phi_2 - \Phi_4$  is externally modulated as  $\Psi_Z = \lambda\Phi_0 \cos(\omega_p t + \phi)$ , where  $\lambda$  is the dimensionless amplitude of the modulation and controls the system-parametric bath coupling strength.

Let  $C_{tl} = cL$  be the capacitance of the TLR, with  $c$  being its capacitance per unit length. Because of the presence of the TLR,  $\Psi_X = \sum_\nu \psi_{\nu L} \sqrt{\frac{\hbar}{2C_{tl}\omega_\nu}}(b_\nu + b_\nu^\dagger)$ . Here,  $\psi_{\nu L}$  is a dimensionless parameter that depends on the boundary conditions at  $z = L$ . For our particular coupling – current-flux – we expect  $\psi_{\nu L} \sim \sin(k_\nu L)$  and, in the weak coupling limit,  $\psi_{\nu L} \propto \nu$ . Ignoring coupling between different transmission line modes, the system Hamiltonian is

$$H_S + H_B + \lambda \cos(\omega_p t + \phi) \sum_\nu h_\nu (b_\nu + b_\nu^\dagger) \Psi_S, \quad (9)$$

where  $h_\nu = \frac{g}{\Phi_0^2} \psi_{\nu L} \sqrt{\frac{\hbar}{2C_{tl}\omega_\nu}}$ . This then directly produces

our model Hamiltonian for generating a chemical potential, where the density of states  $J(\nu) = h(\nu)^2 \rho(\nu) \propto \nu$ , i.e., an Ohmic bath<sup>29</sup>.

For the optical domain, we need a different parametric process. A convenient one is the optomechanical coupling between motion of a mirror and the frequency of light in a cavity formed by the mirror. This example case has been worked in partial detail in Ref.<sup>22</sup>. The key idea is for a pump field to take the radiation pressure coupling  $a^\dagger a x$  to a fast oscillating coupling via  $a \rightarrow a + \alpha e^{-i\omega_p t}$ , producing a parametric coupling to the phonon ‘bath’ with frequency  $\omega_p$ . The details and benefits of this approach will be considered in a separate work.

#### 4. MASTER EQUATION

We consider now what happens to a lattice of coupled, interacting photonic resonators, coupled to both a parametric bath at inverse temperature  $\beta$  and nominal coupling rate  $\gamma$  and to a high frequency (loss) bath with loss rate  $\kappa$ . For simplicity, we consider only strong on-site repulsion  $U$ , and have for the conservative parts of the evolution, a Bose-Hubbard hamiltonian<sup>26</sup> in the rotating frame:

$$\begin{aligned} H_S &= H_0 + H_J \text{ with} \\ H_0 &= \sum_i \left[ \frac{U}{2} n_i(n_i - 1) - \mu n_i \right] \text{ and} \\ H_J &= -J \sum_{\langle ij \rangle} a_i^\dagger a_j \end{aligned}$$

We explicitly derive the master equation for the system, using the usual prescription: first, move to the interaction picture with respect to  $H_S + H_B$ , where  $H_B$  is the bath Hamiltonian and the  $\lambda$  prefactor in the system-bath coupling will be a perturbative parameter. We can write the evolution equation for short times  $\tau$  as

$$\dot{\rho}_I(\tau) = -i\lambda[H_{SB}(\tau), \rho_I(0)] - \lambda^2 \int_0^\tau [H_{SB}(\tau), [H_{SB}(t), \rho_I(t)]] dt$$

with  $H_{SB}(t) = \sum_j B_j(t) x_j(t)$  the system-bath coupling in the interaction picture, writing  $x_j(t) = a_j(t) + a_j^\dagger(t)$ .

Now we make the Born and Markov approximations. That is, we replace  $\rho_I(t)$  with  $\rho_S(\tau) \otimes \rho_B$ . Here  $\rho_B$  is the bath density matrix which will be time-translation invariant for a infinite bath, and is independent of  $\rho_S$  with  $\langle B_i \rangle \equiv \text{Tr}_B[B_i \rho_B] = 0$  for all bath operators coupled to the system. From these two approximations, we can trace over the bath and recover the master equation (in the interaction picture)

$$\begin{aligned} \dot{\rho}_S(\tau) &= - \sum_{ij} \int_0^\infty S_{ij}(t) [x_i(\tau) x_j(\tau - t) \rho_s - x_i(\tau) \rho_S x_j(\tau - t)] \\ &\quad + S_{ij}(-t) [\rho_s x_j(\tau - t) x_i(\tau) - x_j(\tau - t) \rho_S x_i(\tau)] dt \end{aligned} \quad (10)$$

with  $S_{ij}(t) = \lambda^2 \text{Tr}_B[B_i(t)B_j(0)]$  the bath correlation function and where, by taking the initial integration point to  $-\infty$ , we have assumed that bath correlations decay faster than the effective damping they induce – consistent with the Markov approximation.

At this point, we wish to develop a time-local master equation. We express  $x_j(t)$  in the energy eigenbasis of  $H_S$ , with states  $|k\rangle$  and energies  $\epsilon_k$  and an ordering in energy such that  $k' > k \rightarrow \omega_{k'k} \equiv \epsilon_{k'} - \epsilon_k \geq 0$ . Then

$$c_j(t) = \sum_{l>k} e^{-i\omega_{lk}t} x_{j,kl} |k\rangle \langle l|, \quad (11)$$

formally defines an operator that reduces or keeps constant the energy, and  $x_j(t) = c_j(t) + c_j^\dagger(t) + x_0$ , with the last term time-independent and neglected in what follows.

Taking independent, Ohmic baths for each coupling term, we have

$$S_{ij}(t) = \delta_{ij} \frac{\hbar}{\pi} \int_0^\infty J(\omega) [(N_{th}(\omega) + 1)e^{-i\omega t} + N_{th}(\omega)e^{i\omega t}] \quad (12)$$

with  $J(\omega) = \omega e^{-\omega/\omega_c}$ ,  $N_{th}(\epsilon) = 1/[\exp(\beta\epsilon) - 1]$ , where  $\beta$  is the inverse temperature of the parametric bath and  $\omega_c \gg U$  is a high frequency cutoff that is irrelevant to the rest of our calculation. At this point, we get terms in the master equation of the form  $S_{ij}(t)(c_i(\tau)c_j(\tau - t)\rho_S)$  and terms of the form  $S_{ij}(t)(c_i(\tau)c_j^\dagger(\tau - t)\rho_S)$ . The former will have phase evolution at a finite frequency as a function of  $\tau$ , and will be neglected in a rotating wave approximation. The latter will also have such terms, except for those with  $\omega_{kl} = \omega_{k'l'}$ , i.e., energy-degenerate transitions. Keeping only these transitions immediately takes us to the usual golden rule result: transitions with a positive energy difference  $\nu$  occur with a rate  $J(\nu)N_{th}(\nu)$  and transitions with a negative energy difference have the rate  $J(\nu)[N_{th}(\nu) + 1]$ .

Thus, when the energy levels of the system are well resolved, we can derive a super operator describing both photon loss and coupling to the parametric bath. Using the commutation of  $H_S$  with  $N$  (the total photon number), we get transitions from  $k$  to  $l$  with rates that depend on whether the total photon number of the two states differs by +1 or -1 as:

$$\Gamma_{k \rightarrow l}^+ = \gamma (N_{th}(|\epsilon_k - \epsilon_l|) + \Theta(\epsilon_k - \epsilon_l)) \sum_i \left| \langle l | a_i^\dagger | k \rangle \right|^2 \quad (13)$$

$$\Gamma_{k \rightarrow l}^- = [\gamma (N_{th}(|\epsilon_k - \epsilon_l|) + \Theta(\epsilon_k - \epsilon_l)) + \kappa] \sum_i \left| \langle l | a_i | k \rangle \right|^2 \quad (14)$$

where  $\gamma = \gamma_0 \frac{|\epsilon_k - \epsilon_l|}{U}$  for the Ohmic bath case,  $\gamma_0$  represents the overall strength of the coupling, and  $\Theta$  is the Heaviside step function. We have gone back to the physical couplings  $a_i$  rather than the many-body energy lowering operator  $c_j$  in order to make clear the special role loss via the high frequency bath plays in Eq. 14.

The superoperator takes Lindblad form with these rates leading to a rate equation in the energy eigenbasis. Solving this numerically for a case of four coupled sites (Fig. 3), we can immediately see an intuitive understanding of the two types of decay processes. The first type, which increase photon number, correspond to the decay of holes (if the energy of the higher photon number state is lower in the rotating frame) or the creation of particles (if otherwise). The second type decreases photon number, and includes both creation of holes via loss and via the parametric bath; consequently, we expect a greater rate for the second process, which will lead to a particle-hole temperature asymmetry as shown below. The simulations themselves correspond to fixing a maximum total particle number per site, finding the eigenenergies of the dissipation-free model, calculating the decay rates in eqs. 13,14, determining the steady state of the master equation, and for that steady state, finding the probability of each state (shown in the inset to Fig. 3), and estimating the Mandel  $Q$  parameter and the average hopping  $\langle a \rangle \equiv \sqrt{|\langle a_i^\dagger a_j \rangle|}$  (shown in Fig. 4).

## 5. STRONG INTERACTION EXPANSION

We now take a simpler form of the superoperator describing both photon loss and coupling in the case of a single resonator site ( $J = 0$ ) to get an analytical handle on the process. That is, we evaluate Eqns. 13,14 in the single site case. Specifically, defining  $E_0(n) = \frac{U}{2}n(n-1) - \mu n$ , the sign of  $\Delta E(n) = E_0(n+1) - E_0(n) = nU - \mu$  determines both the direction of decay and the thermal bosonic enhancement factor  $N_{th}(|\Delta E(n)|)$ . Thus  $\Gamma_{n \rightarrow n+1}^+ = \gamma f_+(n)$ ,  $\Gamma_{n+1 \rightarrow n}^- = \kappa + \gamma f_-(n)$  with

$$f_+(n) = (n+1) [N_{th}(|\Delta E(n)|) + \Theta(-\Delta E(n))] , \quad (15)$$

$$f_-(n) = (n+1) [N_{th}(|\Delta E(n)|) + \Theta(\Delta E(n))] . \quad (16)$$

and  $\gamma = \gamma_0 |\Delta E(n)|/U$  for the Ohmic bath case. The change from  $N_{th}$  to  $N_{th} + 1$  that occurs in these two factors with the change in sign of  $\Delta E(n)$  arises from having both co- and counter-rotating terms in the system bath coupling.

One consequence of the strong interaction (sometimes called strong coupling in the Mott insulator literature) limit ( $J \rightarrow 0$ ) is an analytical form for the steady state. Specifically, we recover a form of detailed balance, where the probability of a transition on a site from photon number  $n$  to  $n+1$  is given by  $\gamma f_+(n)$  while the transition from  $n+1$  to  $n$  is  $\gamma f_-(n) + (n+1)\kappa$ . This gives, in steady state, a set of ratios

$$\frac{p_1}{p_0} = \frac{f_+(0)}{f_-(0) + \kappa/\gamma} \quad (17)$$

$$\frac{p_2}{p_1} = \frac{f_+(1)}{f_-(1) + \kappa/\gamma} \quad (18)$$

$$\dots \quad (19)$$

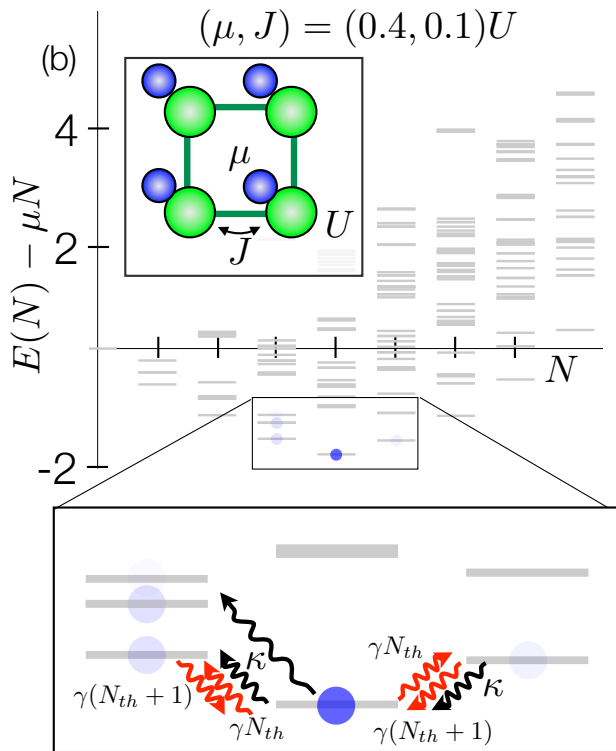


Figure 3: Energy eigenstates plotted as a function of energy and total photon number  $N$  for a numerical solution of a four site Bose-Hubbard model (shown in the upper inset) with  $(J, \mu, \gamma, \kappa) = (0.1, 0.4, 0.01, 0.003)U$  and  $\beta = 1/10U$ . The opacity of the blue dots represent the probability, in steady state, of being in the associated energy eigenstate. The lower inset shows the region near the ground state in the rotating frame; hole-like excitations (lower  $N$ ) are preferentially filled due to optical loss processes  $\kappa$  only reducing particle number. The relatively high temperature leads to some thermal filling of the first particle excited state.

where the correction from a thermal distribution arises from the term  $\kappa/\gamma$ , which depends on the energy difference via  $\gamma$ . We can characterize this for two regimes. First, when  $\Delta E(n)$  is positive (it costs energy to add a photon), we expect the ratio  $p_{n+1}/p_n = N_{eff}^{(p)}/(N_{eff}^{(p)} + 1)$ . This defines the bosonic occupation as seen by particle addition as

$$N_{eff}^{(p)} = \frac{N_{th}(|\Delta E(n)|)}{1 + \kappa/\gamma}$$

Thus, when particles cost energy, photon loss reduces the effective temperature of the system.

Similarly, when  $\Delta E(n)$  is negative, we expect  $p_{n+1}/p_n = (N_{eff}^{(h)} + 1)/N_{eff}^{(h)}$ , which defines the bosonic occupation as seen by hole addition:

$$N_{eff}^{(h)} = \frac{[N_{th}(|\Delta E(n)|) + \kappa/\gamma]}{1 - \kappa/\gamma}$$

Here, photon loss increases the energy, and thus increases the effective temperature of the system. Furthermore, any hope of a thermal description will necessarily break-down for  $\kappa/\gamma \geq 1$ .

Having established that a Mott insulator-like phase emerges from the single site picture, we can ask how the asymmetry of particles and holes changes the standard picture of the edges of the Mott lobes, by using a picture of free particles and holes above the  $n_0$  particle-per-site Mott state  $|\Psi_M\rangle \propto \prod_i (a_i^\dagger)^{n_0} |\text{vac}\rangle$ , i.e., using small  $J$  perturbation theory in the strong interaction limit. A crucial difference from the standard treatment<sup>33</sup> is the use of an implicit finite lifetime to such excitations due to the coupling to both parametric and high frequency baths.

When  $J$  exceeds damping and dephasing, we can no longer use a master equation appropriate to a single site. Specifically, as we want the parametric bath to resolve the kinetic terms in the Hamiltonian, we require  $\gamma [= \gamma_0(J/U)] \ll J$ . We can, however, characterize the dilute limit (where particle hole collisions are neglected) by using our  $N_{eff}^{(p[h])}$ , and we can ask over what domain of parameter space is the combined occupation of particles and holes small compared to one per site. Here we rely upon the standard picture of particle and hole energies to order  $J^2/U$ , neglecting loss-induced changes to the energy differences, consistent with  $\kappa \leq \gamma \ll J$ . The energy of a particle(hole) of wave vector  $k = 0$  above the Mott state is given by Ref.<sup>33</sup> and reproduced here to order  $J^2/U$ :

$$\Delta E^{(p)} = -zJ(n_0 + 1) + n_0U - \mu + \frac{zJ^2}{2U}n_0(5n_0 + 4) - \frac{z^2J^2}{U}n_0(n_0 + 1) \quad (20)$$

$$\Delta E^{(h)} = -zJ(n_0) - (n_0 - 1)U + \mu + \frac{zJ^2}{2U}(n_0 + 1)(5n_0 + 1) - \frac{z^2J^2}{U}n_0(n_0 + 1) \quad (21)$$

where  $z$  is the number of nearest neighbors.

We can then calculate the average particle and hole

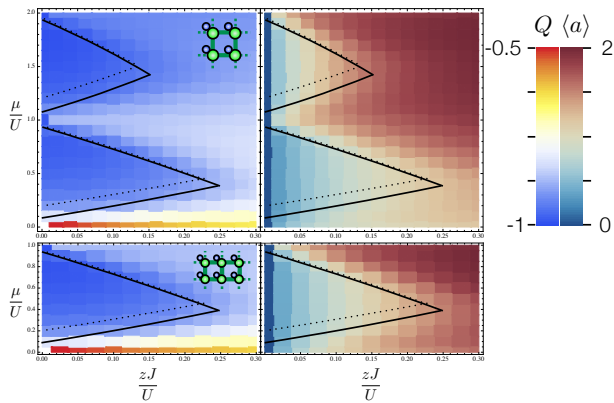


Figure 4: Numerical results for Mandel  $Q$  (left) and coherence  $\langle a \rangle \equiv \sqrt{|\langle a_i^\dagger a_j \rangle|}$  (right) using the four-site (top) and a six-site (bottom) Bose-Hubbard model with periodic boundary conditions. We assume an Ohmic parametric bath and a flat high frequency (loss) bath. The Mandel  $Q \approx -1$  regions (dark blue, left plot) are the Mott insulator states; at the same time, the finite coherence between sites on the right indicates the emergence of superfluid order (right plot) outside the Mott lobes. Finite size effects prevent observation of sharp transitions. Here  $\gamma_0 = 0.07U$  and  $\kappa = \gamma_0/30$ . Overlaid are the critical values for finite occupation of particles and holes (solid black lines), with the dotted line for a higher value of  $\kappa = \gamma_0/3$ . The asymmetry of particles and holes arises due to preferential hole creation from optical loss.

expectation values including both the parametric bath and the high frequency (photon loss) bath, and find that these lowest energy modes have just  $N_{eff}^{(p)}$  and  $N_{eff}^{(h)}$  with the above  $\Delta E^{(p|h)}$ . The boundary of the phase would then correspond to this effective occupation approaching unity (at which point we make expect a macroscopic occupation of particles and/or holes in the system, taking us far from the Mott state). This boundary is shown for two different values of  $\kappa/\gamma_0$  in Fig. 4; as  $\kappa$  increases, the lobes become asymmetric, consistent with additional hole creation via particle losses.

We now consider what near equilibrium picture can emerge, and in particular focus on a picture with two reservoirs (particles and holes) at different temperatures due to loss into the high frequency bath. In the limit of  $\kappa \rightarrow 0$ , we recover the usual picture of an equilibrium system, and get a critical temperature defined as

$$T_c^{(0)} = \frac{1}{k_B \log 2} \text{Min}[\Delta E^{(h)}, \Delta E^{(p)}]$$

However, including the non equilibrium effects, we instead have for the parametric bath temperature the requirement

$$T \leq T_c^{(ne)} = \frac{1}{k_B} \text{Min} \left[ \frac{\Delta E^{(h)}}{\log \left( \frac{2(\gamma^h - \kappa)}{\gamma^h - 2\kappa} \right)}, \frac{\Delta E^{(p)}}{\log \left( \frac{2\gamma^p + \kappa}{\gamma^p + \kappa} \right)} \right] \quad (22)$$

where  $\gamma^{h[p]}$  depends on  $\Delta E^{(h[p])}$  via  $J(\omega)$ .

Further analysis of the particle-hole picture at finite temperature will no doubt elucidate additional physics for this non equilibrium system, following perhaps the efforts of Refs.<sup>34,35</sup>. In addition, an appropriate mean field theory including modifications of the system-bath coupling could provide insight into the applicability of such theories for describing non-equilibrium systems.

## 6. CONCLUSION

Providing a robust chemical potential for light allows for classical and quantum systems to access a wide variety of heretofore forbidden domains. Crucially, our approach allows one to build from well established theoretical tools for non equilibrium problems with chemical potential imbalances, such as occurs in circuits and cold atom systems, rather than the thornier problems associated with driven steady-state systems more typical to the quantum optical domain. From a quantum simulation perspective, this simplification makes the state preparation problem much more straightforward than existing approaches, and yields a mechanism for robust quantum simulation of condensed matter and chemistry problems with light. In addition, our parametric coupling scheme has a wide range of potential implementations, all of which are accessible with current technology, and enables a variety of practical applications in the context of non-classical sources in the microwave and optical domain that operate more in analogy to a diode than to a pumped dissipative steady-state system.

We thank S. Girvin, A. Houck, B. L. Hu, J. Keeling, J. Freericks, M. Devoret, E. Kapit, and P. Zoller for helpful discussions. Support was provided by the NSF-funded Physics Frontier Center at the JQI and by ARO MURI award W911NF0910406.

<sup>1</sup> Planck, M. The Theory of Heat Radiation. P. BLAKISTON'S SON & CO. (1914).

<sup>2</sup> Wurfel, P. The chemical potential of radiation. *Journal of Physics C: Solid State Physics* **15**, 3967–3985 (1982).

<sup>3</sup> Ries, H. & McEvoy, A. Chemical potential and temperature of light. *Journal of Photochemistry*

and *Photobiology A: Chemistry* **59**, 11 – 18 (1991). URL <http://www.sciencedirect.com/science/article/pii/1010603091870632>.

<sup>4</sup> Herrmann, F. & Wurfel, P. Light with nonzero chemical potential. *American Journal of Physics* **73**, 717–721 (2005). URL <http://scitation.aip.org/content/aapt/>

- journal/ajp/73/8/10.1119/1.1904623.
- <sup>5</sup> Job, G. & Herrmann, F. Chemical potential—a quantity in search of recognition. *European Journal of Physics* **27**, 353 (2006). URL <http://stacks.iop.org/0143-0807/27/i=2/a=018>.
  - <sup>6</sup> Eastham, P. & Littlewood, P. Bose condensation of cavity polaritons beyond the linear regime: The thermal equilibrium of a model microcavity. *Phys. Rev. B* **64**, 235101 (2001).
  - <sup>7</sup> Klaers, J., Schmitt, J., Vewinger, F. & Weitz, M. Bose-Einstein condensation of photons in an optical microcavity. *Nature* **468**, 545–548 (2010).
  - <sup>8</sup> Sun, C. *et al.* Observation of the kinetic condensation of classical waves. *Nat. Phys.* **8**, 471–475 (2012).
  - <sup>9</sup> Klaers, J., Schmitt, J., Damm, T., Vewinger, F. & Weitz, M. Statistical physics of bose-einstein-condensed light in a dye microcavity. *Phys. Rev. Lett.* **108**, 160403 (2012). URL <http://link.aps.org/doi/10.1103/PhysRevLett.108.160403>.
  - <sup>10</sup> Snoke, D. & Girvin, S. Dynamics of phase coherence onset in bose condensates of photons by incoherent phonon emission. *Journal of Low Temperature Physics* **171**, 1–12 (2013). URL <http://dx.doi.org/10.1007/s10909-012-0854-6>.
  - <sup>11</sup> Yukalov, V. I. Difference in bose-einstein condensation of conserved and unconserved particles. *LASER PHYSICS* **22**, 1145–1168 (2012).
  - <sup>12</sup> Angelakis, D., Santos, M. & Bose, S. Photon-blockade-induced mott transitions and xy spin models in coupled cavity arrays. *Phys. Rev. A* (2007).
  - <sup>13</sup> Greentree, A. D., Tahan, C., Cole, J. H. & Hollenberg, L. C. L. Quantum phase transitions of light. *Nat. Phys.* (2006).
  - <sup>14</sup> Hartmann, M. J., Brandao, F. G. S. L. & Plenio, M. B. Strongly interacting polaritons in coupled arrays of cavities. *Nat. Phys.* (2006).
  - <sup>15</sup> Chang, D. E. *et al.* Crystallization of strongly interacting photons in a nonlinear optical fibre. *Nat. Phys.* (2008).
  - <sup>16</sup> Hafezi, M., Chang, D., Gritsev, V., Demler, E. & Lukin, M. Quantum transport of strongly interacting photons in a one-dimensional nonlinear waveguide. *Phys. Rev. A* (2012).
  - <sup>17</sup> Carusotto, I. *et al.* Fermionized Photons in an Array of Driven Dissipative Nonlinear Cavities. *Phys. Rev. Lett.* (2009).
  - <sup>18</sup> Carusotto, I. & Ciuti, C. Quantum fluids of light. *REVIEWS OF MODERN PHYSICS* **85** (2013).
  - <sup>19</sup> Kassal, I., Jordan, S. P. & Love, P. J. Polynomial-time quantum algorithm for the simulation of chemical dynamics. *PNAS* 18681–18686 (2008).
  - <sup>20</sup> Jordan, S. P., Lee, K. S. M. & Preskill, J. Quantum Algorithms for Quantum Field Theories. *Science* **336**, 1130–1133 (2012).
  - <sup>21</sup> Buluta, I. & Nori, F. Quantum Simulators. *Science* **326**, 108–111 (2009).
  - <sup>22</sup> Weitz, M., Klaers, J. & Vewinger, F. Optomechanical generation of a photonic bose-einstein condensate. *Phys. Rev. A* **88**, 045601 (2013). URL <http://link.aps.org/doi/10.1103/PhysRevA.88.045601>.
  - <sup>23</sup> de Leeuw, A.-W., Stoof, H. T. C. & Duine, R. A. Schwinger-keldysh theory for bose-einstein condensation of photons in a dye-filled optical microcavity. *Phys. Rev. A* **88**, 033829 (2013). URL <http://link.aps.org/doi/10.1103/PhysRevA.88.033829>.
  - <sup>24</sup> Sob'yanin, D. N. Bose-einstein condensation of light: General theory. *Phys. Rev. E* **88**, 022132 (2013). URL <http://link.aps.org/doi/10.1103/PhysRevE.88.022132>.
  - <sup>25</sup> Kirton, P. & Keeling, J. Nonequilibrium model of photon condensation. *Phys. Rev. Lett.* **111**, 100404 (2013). URL <http://link.aps.org/doi/10.1103/PhysRevLett.111.100404>.
  - <sup>26</sup> Fisher, M., Weichman, P. B., Grinstein, G. & Fisher, D. S. Boson localization and the superfluid-insulator transition. *Phys. Rev. B* **40**, 546–570 (1989).
  - <sup>27</sup> Subaşı, Y., Fleming, C. H., Taylor, J. M. & Hu, B. L. Equilibrium states of open quantum systems in the strong coupling regime. *Phys. Rev. E* (2012).
  - <sup>28</sup> Devoret, M. *Quantum fluctuations in electrical circuits* (Les Houches, Session LXIII, 1995).
  - <sup>29</sup> Clerk, A. A., Devoret, M. H., Girvin, S. M., Marquardt, F. & Schoelkopf, R. J. Introduction to quantum noise, measurement, and amplification. *Rev. Mod. Phys.* **82**, 1155 (2010).
  - <sup>30</sup> Bergeal, N. *et al.* Phase-preserving amplification near the quantum limit with a Josephson ring modulator. *Nature* (2010).
  - <sup>31</sup> Bergeal, N. *et al.* Analog information processing at the quantum limit with a josephson ring modulator. *Nat Phys* **6**, 296–302 (2010). URL <http://dx.doi.org/10.1038/nphys1516>.
  - <sup>32</sup> Abdo, B., Kamal, A. & Devoret, M. Nondegenerate three-wave mixing with the Josephson ring modulator. *Phys. Rev. B* **87**, 014508 (2013).
  - <sup>33</sup> Freericks, J. & Monien, H. Phase diagram of the Bose-Hubbard Model. *EPL (Europhysics Letters)* **26**, 545–550 (1994).
  - <sup>34</sup> Capogrosso-Sansone, B., Trefzger, C., Lewenstein, M., Zoller, P. & Pupillo, G. Quantum Phases of Cold Polar Molecules in 2D Optical Lattices. *Phys. Rev. Lett.* (2010).
  - <sup>35</sup> Gupta, M., Krishnamurthy, H. R. & Freericks, J. K. Strong-coupling expansion for ultracold bosons in an optical lattice at finite temperatures in the presence of superfluidity. *Phys. Rev. A* **88**, 053636 (2013).